ELSEVIER

Vlaams Instituut voor de Zee
Flanders Marine Institute

Journal of Marine Systems 31 (2002) 279–297

JOURNAL OF MARINE SYSTEMS

www.elsevier.com/locate/jmarsys

The concept of age in marine modelling II. Concentration distribution function in the English Channel and the North Sea

Éric J.M. Delhez [a,*], Éric Deleersnijder [b,c]

[a] *Université de Liège, Mathématiques Générales, Sart-Tilman B37, B-4000 Liège, Belgium*
[b] *Institut de Recherche Mathématique de Rennes, Université Rennes 1, CS 74205, F-35042 Rennes Cedex, France*
[c] *Université Catholique de Louvain, Institut d'Astronomie et de Géophysique G. Lemaître, Chemin du Cyclotron 2, B-1348 Louvain-la-Neuve, Belgium*

Received 29 March 2001; accepted 7 September 2001

Abstract

The age of seawater and the age of real or idealized tracers are often used as diagnostic tools to better understand complex hydrodynamic flows. In most studies, the focus is on some averages of the ages of the different particles making up a water parcel. The theory developed in Delhez et al. [Ocean Modell. 1 (1999) 17] and Deleersnijder et al. [J. Mar. Syst. 28 (2001) 229] provides, however, a more detailed description of the distribution of the ages of these particles through the so-called concentration distribution function. In this paper, the numerical aspects of the resolution of the evolution equation for the concentration distribution function in a five-dimensional space (time × 3D space × age dimension) are developed. Evolution equations for the moments of the concentration distribution function up to any order are also derived. A real case application of this theory to the simulation of the advection–dispersion of tracers (technetium-99) discharged at the nuclear fuel reprocessing plant of Cap de La Hague is described. The comparison of the results with those from previous studies demonstrates the advantages of the new method for the computation of the mean age. In particular, the method provides a detailed description of the temporal variations of the mean age only. The analysis of the full concentration distribution function and of its basic statistics shows that the standard deviation of the age of the different particles is far from negligible and should never be overlooked when analyzing age fields. A simplified analytical example suggests that the standard deviation of the age distribution is a measure of the integrated diffusion undergone by the tracer along its path from the source to the observation point.

Keywords: Age; Age of seawater; Radioisotope; Tracer; English Channel; North Sea; Concentration distribution function

1. Introduction

The concept of the "age of a water parcel"—together with its extensions to the "age of a water mass" or the "age of a constituent" and the likes—is widely used in ocean sciences to highlight the inherent time scales of a system associated with the advection–diffusion of mat-

* Corresponding author. Université de Liège, Mathématiques Générales, Sart-Tilman B37, B-4000 Liège, Belgium. Tel.: +32-4-366-9419/9347; fax: +32-4-366-9489.
E-mail address: E.Delhez@Ulg.ac.be (É.J.M. Delhez).

0924-7963/02/$ - see front matter
PII: S0924-7963(01)00066-5

ter. Here, we will define the age of a parcel of a constituent as the "time elapsed since the parcel under consideration left the region in which its age is prescribed to be zero" (e.g. Zimmerman, 1976; Takeoka, 1984; Delhez et al., 1999a). This definition applies to the study of the horizontal transport of tracers from a given source through shelf seas (e.g. Ostlund, 1994; Prandle, 1984; Dahlgaard, 1995; Rutgers Van der Loeff et al., 1995; Salomon et al., 1995; Turekian et al., 1996; Delhez and Carabin, in press), as well as to the study of the rate of ventilation of the deep ocean (e.g. Jenkins and Clarke, 1976; Thiele and Sarmiento, 1990; Broecker et al., 1990; England, 1995; England and Holloway, 1998; Haine et al., 1998; Campin et al., 1999).

While the age of a single particle can be defined and interpreted unambiguously, the case is much more difficult when considering the age of a water mass or even of a set of particles because the ages of the different particles are then a priori different. With the usual techniques of the radioactive dating, i.e. ^{14}C technique, $^{3}H/^{3}He$ ratio (e.g. Jenkins and Clarke, 1976; Broecker et al., 1990; Campin et al., 1999), or of the labeling of water masses by two or more tracers of known history of release, i.e. CFC-11/CFC-12, CCl_4/F-11 ratios (e.g. England and Holloway, 1998; Haine et al., 1998), only a certain mean age is accessible experimentally. The same limitation applies to the numerical methods of determination of age that mimic these experimental techniques: only an loosely defined "average age" of the water parcels is available.

Previous papers have already highlighted the fact that mixing introduces a bias in the age determined by means of the techniques mentioned above (e.g. Jenkins, 1987; Thiele and Sarmiento, 1990; England and Holloway, 1998; Delhez et al., 1999a; Deleersnijder et al., 2001a; Khatiwala et al., 2001). The aim of this paper is to show that mixing raises also the problem of the significance of the mean age as a characterization of the full age dis-tribution and to show how the general theory of age developed in Delhez et al. (1999a) and Deleersnijder et al. (2001a) can be used to tackle this issue.

2. The concentration distribution function

The concept of a concentration or age density function has been used, sometimes with different names, in both theoretical and case studies (e.g. Bolin and Rodhe,1973; Zimmerman, 1976; Takeoka, 1984, Beining and Roether, 1996; Hall and Plumb, 1994; Delhez et al., 1999a, Holzer and Hall, 2000; Deleersnijder et al., 2001a). As detailed in Delhez et al. (1999a), the idea is simply to split the concentration of a tracer into continuous age classes: the concentration distribution function $c(t, \mathbf{x}, \tau)$ represents then the contribution of the material with an age of τ to the total concentration $C(t, \mathbf{x})$ of that tracer so that

$$C(t, \mathbf{x}) = \int_0^\infty c(t, \mathbf{x}, \tau)\mathrm{d}\tau \tag{1}$$

i.e. the concentration distribution function is the density function describing the distribution of the concentration in the age space (Fig. 1, second panel).

Delhez et al. (1999a) showed that c satisfies the partial differential equation

$$\frac{\partial c}{\partial t} + \mathbf{v}\cdot\nabla c + \frac{\partial c}{\partial \tau} = p - d + \nabla\cdot(\mathbf{K}\cdot\nabla c) \tag{2}$$

where ∇ is the nabla/del vector differential operator in the physical space, p and d are, respectively, the local production and destruction rates of material of age τ, $\mathbf{v}$ is the current vector and $\mathbf{K}$ is the eddy diffusivity tensor.

The mean age a is related to the first-order moment of the concentration distribution function (Delhez et al., 1999a; Deleersnijder et al., 2001a) through

$$a(t, \mathbf{x}) = \frac{1}{C(t, \mathbf{x})}\int_0^\infty \tau c(t, \mathbf{x}, \tau)\mathrm{d}\tau \tag{3}$$

Evolution equations for the total concentration $C(t, \mathbf{x})$ and the age concentration $\alpha(t, \mathbf{x}) = a(t, \mathbf{x})C(t, \mathbf{x})$ are easily derived from Eq. (2) (Delhez et al., 1999a):

$$\frac{\partial C}{\partial t} + \mathbf{v}\cdot\nabla C = \int_0^\infty p\mathrm{d}\tau - \int_0^\infty d\ \mathrm{d}\tau + \nabla\cdot(\mathbf{K}\cdot\nabla C) \tag{4}$$

$$\frac{\partial \alpha}{\partial t} + \mathbf{v}\cdot\nabla\alpha = C + \int_0^\infty \tau p\mathrm{d}\tau - \int_0^\infty \tau d\ \mathrm{d}\tau + \nabla\cdot(\mathbf{K}\cdot\nabla\alpha) \tag{5}$$

Eq. (1) must be solved in a five-dimensional space (time × 3D space × age dimension).

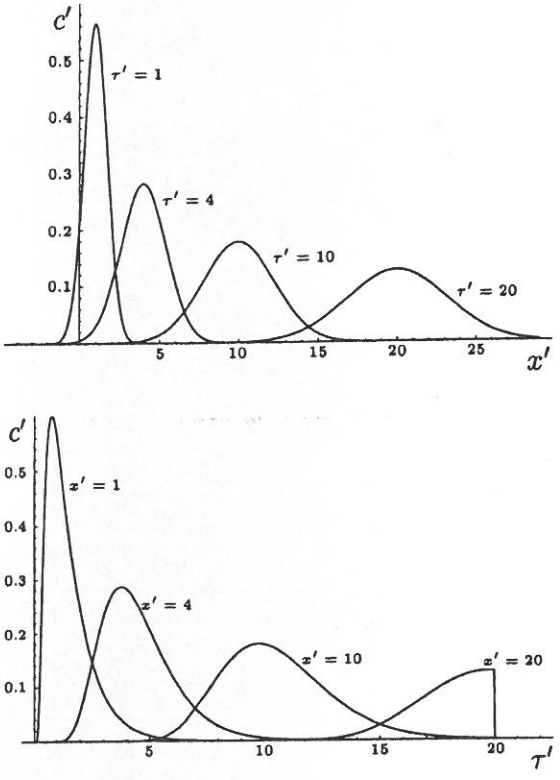

Fig. 1. Dimensionless concentration distribution function c' at $t'=20$ for $\tau'=1$, 4, 10 and 20 (first panel) and $x'=1$, 4, 10 and 20 (second panel) for a constant release starting at $t'=0$.

Considering that the age is positive definite, as implicitly assumed in expressions (1) and (2), the boundary condition at $\tau=0^-$ is simply:

$$c(t,\ \mathbf{x},\ 0^-)=0 \tag{6}$$

The distinction is made between 0^- and 0^+ because of the possibility of a discontinuity of the concentration distribution function at 0 associated with a source of new material. Such a source can be taken into account by including an appropriate Dirac function in the production term p.

The initial and boundary conditions to be prescribed at physical interfaces, as well as the production and destruction terms depend on the constituent, on the application and on the features that one wants to highlight.

In a study of the spreading of a pollutant injected into the system through a physical interface, the age of the incoming material will usually be prescribed to be zero. This defines the age as the time elapsed since the material entered the marine system. The boundary condition is then expressed as

$$\mathbf{q}\cdot\mathbf{n}\equiv(\mathbf{v}c-\mathbf{K}\cdot\nabla c)\cdot\mathbf{n}=-J\delta(\tau) \tag{7}$$

where J is the prescribed incoming flux of pollutant, δ is the Dirac impulsion, $\mathbf{n}$ is the outward unit vector normal to the boundary of the marine domain and $\mathbf{q}$ denotes the advection + diffusion flux (the minus sign appears because $\mathbf{q}$ and $\mathbf{n}$ have opposite directions for an input flux).

If some new material is produced in the ocean interior, through chemical reactions or biological processes for instance, the age of this new material will be set to zero at the time of its production. Consequently, the concentration distribution function will reflect the concentration and the time spent by the different parcels in the system since their synthesis. For a point source located at $\mathbf{x}_S$, the production term will then appear as

$$p=S\delta(\mathbf{x}-\mathbf{x}_S)\delta(\tau-\tau_S) \tag{8}$$

where S is the strength of the source and $\tau_S=0$ (a value of τ_S different from zero can be used for other purposes to represent the production of material with a given age).

For the assessment of the ventilation time scale of a closed basin, age is understood as the time elapsed since the particles were last exposed to the surface. In this case, Eq. (2) is solved using the boundary condition

$$c(t,\ \mathbf{x}_{\mathrm{Surf}},\ \tau)=1\ \delta(\tau) \tag{9}$$

which is equivalent to the introduction of an artificial tracer that marks the water masses that were once exposed to the surface (its concentration is conveniently set to 1 at the surface) and to the prescription of the age of this artificial tracer to zero at the surface, in agreement with the definition of the age in such a study.

3. Concentration distribution function—a 1D analytical example

To develop a more intuitive understanding of the concentration distribution function, it is useful to

consider the idealized case of a one-dimensional problem within an infinite domain $x\in]-\infty,\infty[$ (i.e. a slightly modified version of the idealised problem considered in Deleersnijder et al., 2001a).

Let us consider a conservative tracer injected at the origin ($x=0$) at a variable rate $J(t)$. Let us further assume that the hydrodynamic conditions are characterized by constant and uniform velocity u and diffusion coefficient κ. For fixed t and τ, $c(t, x, \tau)$ (in this section we will drop the subscript i) simply describes the spatial distribution of the tracer released at time $t-\tau$. The solution of Eq. (2) is, therefore, easily computed from the classical solution of the 1D advection–diffusion equation as

$$c(t,\ x,\ \tau)=\frac{J(t-\tau)}{\sqrt{4\pi\kappa\tau}}\exp\left[-\frac{(x-u\tau)^2}{4\kappa\tau}\right] \tag{10}$$

This equation shows that, as assumed in Eq. (27), the concentration distribution function decreases exponentially to zero for large τ provided that u is not zero. In a case of pure diffusion, the concept of age is, therefore, not applicable (Beining and Roether, 1996) unless the flux $J(t)$ is nonzero only during a finite period of time. In particular, no steady state solution can be obtained (in terms of age) with pure diffusion.

One verifies easily that

$$\int_{-\infty}^{\infty}c(t,\ x,\ \tau)\mathrm{d}x=J(t-\tau) \tag{11}$$

in accordance with the above interpretation of the concentration distribution function.

The concentration distribution function (Eq. (10)) is shown in Fig. 1 for a constant release $J(t)=J_0h(t)$ (where J_0 is a constant and $h(t)$ is the Heaviside step-function) from time $t=0$ onwards using the dimensionless variables

$$t'=\frac{u^2}{4\kappa}t,\quad x'=\frac{u}{4\kappa}x,$$

$$\tau'=\frac{u^2}{4\kappa}\tau,\quad c'=\frac{4\kappa}{J_0u}c \tag{12}$$

The spatial distribution of the concentration distribution function is characterized by a continuum of symmetrical patches of tracer that have been advected at the (constant) velocity u and that have undergone spatial diffusion for a period of time τ. Of course, older patches are much smoother than younger patches. In the extreme case with no diffusion, c degenerates into a series of Dirac pulses.

The dependency of the distribution function on the age τ can be explained as follows. In the vicinity of the source, the main contribution to the tracer concentration is made of material that has been released rather recently in the system. The concentration distribution function shows, therefore, a clear maximum and a long tail on the side of the larger ages. At a larger distance, the tracer concentration is a mixture of young and old material with a maximum corresponding to the advection time scale from the source. With the constant release starting at $t=0$ considered here, there is of course no material older than time t. Consequently, the concentration distribution function shows a cut-off at $\tau=t$ that becomes more and more evident far from the source.

One can notice that because of the parabolic nature of the advection–diffusion equation, newly injected tracer can be found immediately at every location, even at remote distances from the source.

Even in the simple set-up considered here, the concentration distribution function is not Gaussian and is not even symmetrical with respect to τ. It is, therefore, poorly characterized by its average value and the mean age gives only a vague account of the real age structure.

From Eq. (10), one can also compute the total concentration and mean age by Eqs. (1) and (3). These are shown in Fig. 2 using the dimensionless variables

$$a'=\frac{u^2}{4\kappa}a,\quad C'=\frac{(4\kappa)^2}{J_0u^3}C \tag{13}$$

As pointed out by Beckers et al. (2001) and Deleersnijder et al. (2001b), the mean age behaves asymptotically as

$$a(t,\ x)\approx\frac{|x|}{u}\ \text{for large } t \tag{14}$$

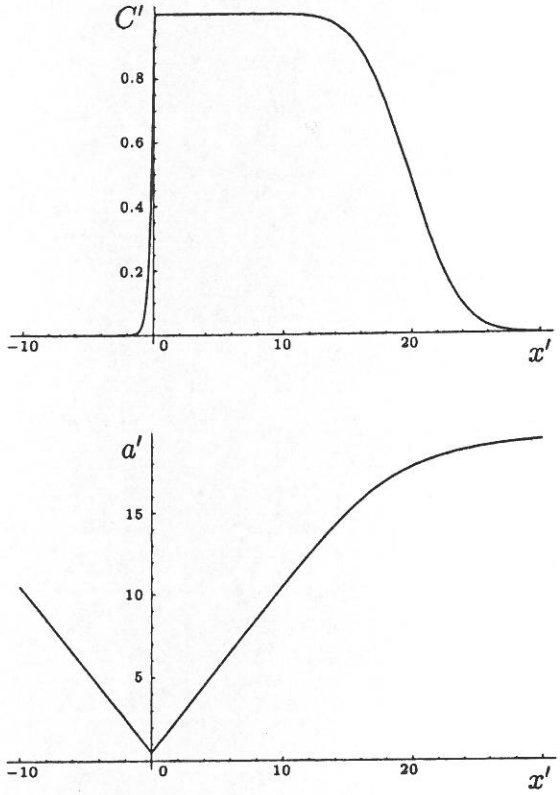

Fig. 2. Dimensionless total concentration C' (first panel) and mean age a' (second panel) at time $t'=20$ for a constant release starting at $t'=0$.

(provided that $u \neq 0$) and tends, therefore, to be independent of the diffusion coefficient! Even for finite and small t, the mean age has the counter-intuitive property to be symmetrical with respect to the source—while the total concentration field itself is, of course, not symmetrical (Beckers et al., 2001; Deleersnijder et al., 2001b). The analysis of the concentration distribution function allows us to complement that conclusion.

First, we introduce the expression "age distribution" to refer to the shape of the concentration distribution function as a function of τ, i.e. to the relative contributions of the different age classes to the total concentration. Mathematically, the age distribution $\tilde{c}$ can be defined as the distribution function normalized by the total concentration, i.e.

$$\tilde{c}(t,\ \mathbf{x},\ \tau) = \frac{c(t,\ \mathbf{x},\ \tau)}{C(t,\ \mathbf{x})} \tag{15}$$

Using Eq. (10), the age distribution in our idealized 1D problem is given by

$$\begin{aligned}\tilde{c}(t,\ x,\ \tau) &= \frac{c(t,\ x,\ \tau)}{C(t,\ x)} \\ &= \frac{\dfrac{J(t-\tau)}{\sqrt{4\pi\kappa\tau}}\exp\left[-\dfrac{(x-u\tau)^2}{4\kappa\tau}\right]}{\displaystyle\int_0^\infty \frac{J(t-\tau)}{\sqrt{4\pi\kappa\tau}}\exp\left[-\frac{(x-u\tau)^2}{4\kappa\tau}\right]\mathrm{d}\tau} \\ &= \frac{\dfrac{J(t-\tau)}{\sqrt{4\pi\kappa\tau}}\exp\left[-\dfrac{x^2+u^2\tau^2}{4\kappa\tau}\right]}{\displaystyle\int_0^\infty \frac{J(t-\tau)}{\sqrt{4\pi\kappa\tau}}\exp\left[-\frac{x^2+u^2\tau^2}{4\kappa\tau}\right]\mathrm{d}\tau}\end{aligned} \tag{16}$$

One gets, therefore, that

$$\tilde{c}(t,\ -x,\ \tau) = \tilde{c}(t,\ x,\ \tau), \tag{17}$$

i.e. not only the mean age is symmetrical, but the whole age distribution (not the concentration distribution function) is symmetrical about the origin whatever the actual release rate $J(t)$. Consequently, the age distribution cannot be used to discriminate between the upwind and downwind directions of the flow, at least in the idealised system considered here.

4. Numerical computation of the concentration distribution

In most realistic cases, Eq. (2) cannot be solved analytically and numerical solutions must be computed.

In the particular case of the steady state solution of Eq. (2) under constant hydrodynamic conditions, Beckers et al. (2001) point out that Eq. (2) reduces to

$$\frac{\partial c}{\partial \tau} + \mathbf{v}\cdot\nabla c = p - d + \nabla\cdot(\mathbf{K}\cdot\nabla c) \tag{18}$$

and is similar to the usual differential equation describing the evolution in space and time of the concentration field of a constituent where time t is replaced by τ. With appropriate boundary and "initial" conditions, the steady state concentration distribution can, thus, be obtained as the transient solution of a

classical advection–diffusion problem using standard resolution techniques.

Under unsteady hydrodynamic conditions, the solution to Eq. (2) can be obtained by a slight modification of the advection–dispersion solver used in the hydrodynamic numerical model. The structure of Eq. (2) is indeed similar to that of an usual advection–diffusion equation with the exception of the ageing term, i.e. the partial derivative of c with respect to age. This term can be considered as an advection term towards larger ages and, hence, discretized with the techniques usually applied to advection terms. Eq. (2) is, thus, solved as an evolution equation in a four-dimensional space (3D space × age). An operator splitting techniques can also be used to handle separately the advection terms in the physical space and the ageing term.

If a finite difference or a finite volume technique is used, the resolution involves not only the discretization of Eq. (2) on the usual three-dimensional grid but also in the age space by splitting the age domain $\tau\in[0, \tau_{max}]$ (where τ_{max} is the maximum age retained in the discretization) into an appropriate number of age classes.

Taking advantage of the "constant velocity" associated with the ageing term, one can also avoid the discretization of this term and the associated errors by introducing the change of variables

$$(t,\ \tau) \rightarrow (\tilde{t} = t,\ \tilde{\tau} = t - \tau) \tag{19}$$

With Eq. (19), one gets indeed

$$\frac{\partial c}{\partial t} + \frac{\partial c}{\partial \tau} + \ldots \rightarrow \frac{\partial c}{\partial \tilde{t}} + \ldots \tag{20}$$

so that there is no differential terms in the τ direction any more. The resolution amounts then to the resolution of a number of classical advection–dispersion equations corresponding to the different discrete age classes considered. These are uncoupled unless the production and destruction terms of the different age classes depend on each other.

To clarify the procedure, let us consider a tracer injected, at any variable or constant rate $J(t)$, into the marine system through one of its boundaries. We define the age as the time elapsed since that material entered the marine system. One starts with dividing the modified age domain $\tilde{\tau}\in[0, \tau_{max}]$ into as many age classes as wanted, say N, so that $\tau_{max} = N\Delta\tau$, where $\Delta\tau$ is the resolution in the age direction. We note $C_k(t, \mathbf{x})$ the integrated content of the kth age class in the transformed $\tilde{\tau}$ age space, i.e.

$$C_k(\tilde{t},\ \mathbf{x}) = \int_{(k-1)\Delta\tau}^{k\Delta\tau} c(\tilde{t},\ \mathbf{x},\ \tilde{\tau})\mathrm{d}\tilde{\tau} \tag{21}$$

that verifies

$$\frac{\partial C_k}{\partial \tilde{t}} + \mathbf{v}\cdot\nabla C_k = \int_{(k-1)\Delta\tau}^{k\Delta\tau} (p-d)\mathrm{d}\tilde{\tau} + \nabla\cdot(\mathbf{K}\cdot\nabla C_k) \tag{22}$$

For $\tilde{t}$ in $[0, \Delta\tau]$, the evolution of C_1 only is computed by solving the discretized version of Eq. (22) for $k=1$ subject to the boundary condition

$$(\mathbf{v}C_1 - \mathbf{K}\cdot\nabla C_1)\cdot\mathbf{n} = -J(\tilde{t}) \tag{23}$$

For $\tilde{t}=\Delta\tau$ to $\tilde{t}=2\Delta\tau$, a second age class is considered, i.e. C_2. Consequently, Eq. (22) is solved for $k=1$ and 2 with the boundary conditions

$$\begin{cases} (\mathbf{v}C_1 - \mathbf{K}\cdot\nabla C_1)\cdot\mathbf{n} = 0 \\ (\mathbf{v}C_2 - \mathbf{K}\cdot\nabla C_2)\cdot\mathbf{n} = -J(\tilde{t}) \end{cases} \tag{24}$$

Continuing this procedure, one introduces progressively the different age classes C_1, C_2, C_3, C_4,... into the system (Fig. 3). At any intermediate time $\tilde{t}$, C_k ($\tilde{t}$,

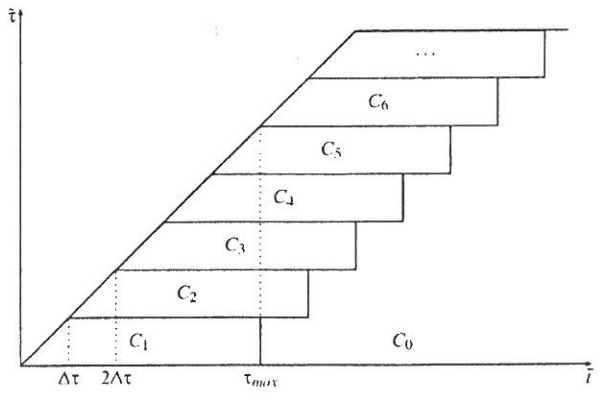

Fig. 3. Schematic representation of the technique used to solve Eq. (2).

$\mathbf{x})$ represents the spatial distribution of the material released between $\tilde{t}=(k-1)\,\Delta\tau$ and $\tilde{t}=k\Delta\tau$, i.e. with an age τ in $[\tilde{t}-(k-1)\Delta\tau,\ \tilde{t}-k\Delta\tau]$.

At time $\tilde{t}=\tau_{\max}$, exactly N age classes have been activated. To go on with the computation without endlessly increasing the number of age classes, one could drop the older age class $C_{k_{\tau max}}$ from the system. We would, however, lose then the tail of the concentration distribution from $\tau=\tau_{\max}$ and higher. To avoid this, an additional age class is introduced to cover the ages τ in $[\tau_{\max},\ \infty[$, i.e.

$$C_0(t,\ \mathbf{x}) = \int_{\tau_{\max}}^{\infty} c(t,\ \mathbf{x},\ \tau)\mathrm{d}\tau \tag{25}$$

As time progresses, the older age classes are then progressively fed into this age class C_0.

Alternatively, the equation for the total concentration field can be solved and the age class C_0 can then be obtained by subtracting the content of the resolved age classes C_k from the total concentration field. This method is used in Section 6. In addition, the resolution of Eq. (5) for the age concentration allows the direct computation of the mean age and can be used to get the mean age of the material forming the tail of the concentration distribution function.

5. Higher-order moments of the concentration distribution function

As an alternative to the full determination of the concentration distribution function, it is interesting to notice that important information about the age spectrum can be obtained from Eq. (2) in much the same way as the evolution equation for the mean age is derived (Delhez et al., 1999a; Deleersnijder et al., 2001a).

We assume, as in Delhez et al. (1999a), that

$$\lim_{\tau\to\infty} c(t,\ \mathbf{x},\ \tau) = 0 \tag{26}$$

or, more generally,

$$\lim_{\tau\to\infty} \tau^n c(t,\ \mathbf{x},\ \tau) = 0 \text{ for any } n \geq 0 \tag{27}$$

This means that the age of any individual parcel can be large but remains finite or, at least, that moments μ_n of any order n of the concentration distribution can be defined by

$$\mu_n(t,\ \mathbf{x}) = \int_0^{\infty} \tau^n c(t,\ \mathbf{x},\ \tau)\mathrm{d}\tau \tag{28}$$

Multiplying Eq. (2) by τ^n, where n stands for any natural number, and integrating this expression over the entire age spectrum, equations for the nth-order moment μ_n can be obtained from

$$\frac{\partial \mu_n}{\partial t} + \mathbf{v}\cdot\nabla\mu_n + \int_0^{\infty} \tau^n \frac{\partial c}{\partial \tau}\mathrm{d}\tau = \int_0^{\infty} \tau^n p\mathrm{d}\tau - \int_0^{\infty} \tau^n d\mathrm{d}\tau + \nabla\cdot(\mathbf{K}\cdot\nabla\mu_n) \tag{29}$$

The integration by parts of the ageing term gives

$$\int_0^{\infty} \tau^n \frac{\partial c}{\partial \tau}\mathrm{d}\tau = [\tau^n c]_0^{\infty} - \int_0^{\infty} n\tau^{n-1} c\mathrm{d}\tau = n\mu_{n-1} \tag{30}$$

using Eq. (5). With the additional definitions of the nth-order production and destruction terms

$$p_n = \int_0^{\infty} \tau^n p\,\mathrm{d}\tau \tag{31}$$

$$d_n = \int_0^{\infty} \tau^n d\,\mathrm{d}\tau \tag{32}$$

one gets

$$\frac{\partial \mu_n}{\partial t} + \mathbf{v}\cdot\nabla\mu_n = n\mu_{n-1} + p_n - d_n + \nabla\cdot(\mathbf{K}\cdot\nabla\mu_n) \tag{33}$$

In particular, Eq. (33) for $n=0$ and 1 leads to, respectively, the equations for the total concentration C and for the age concentration.

As a result, moments of the concentration distribution function can be determined up to any order N by solving Eq. (33) for $n=0,1,\ \ldots\ ,N$ provided the corresponding production–destruction terms and boundary conditions can be expressed in an appropriate form.

In practice, the careful design of the numerical scheme is required to take into account the coupling of the equations for the successive moments μ_n through the ageing term and avoid a progressive deterioration of the solution because of the accumulation of numerical errors for increasing orders of μ_n.

From the knowledge of the moments μ_n ($n=0, \ldots, N$), it is then feasible to reconstruct a continuous representation of the concentration distribution function (in the age dimension).

It can be shown that the distribution function $\hat{c}(t, \mathbf{x}, \tau)$ of maximum entropy, i.e. the distribution corresponding to the minimum-bias solution since any other function would introduce a bias with respect to the available information, when the moments up to order N are known is given by

$$\hat{c}(t,\ \mathbf{x},\ \tau) = \exp\left[\sum_{k=0}^{N} \lambda_k \tau^k\right] \tag{34}$$

where λ_k ($k=0, \ldots, N$) are appropriate functions of time and space (e.g. Tou and Gonzalez, 1974). When $N=2$, however, i.e. when only the mean age and the variance are known, Eq. (34) produces a Gaussian while it was clear in the 1D analytical example that the distribution at given time and location is not Gaussian in general and is not even symmetrical. Therefore, it is then better to fit an expression like

$$\hat{c}(t,\ \mathbf{x},\ \tau) = \frac{\gamma}{\sqrt{\pi\beta^2\tau}} \exp\left[-\left(\sqrt{\frac{\alpha^2}{\tau}} - \sqrt{\frac{\tau}{\beta^2}}\right)^2\right] \tag{35}$$

inspired from Eq. (10), where $\alpha(t, \mathbf{x})$, $\beta(t, \mathbf{x})$ and $\gamma(t, \mathbf{x})$ are worked out to satisfy the constraints

$$\int_0^\infty \tau^n \hat{c}\,\mathrm{d}\tau = \mu_n \quad (n = 0,\ 1,\ 2) \tag{36}$$

In this way, the numerical computation of $\mu_0 = C$, $\mu_1 = \alpha$ and μ_2 can appear as a cheap alternative to the computation of the full concentration distribution function. This should, however, be restricted to simple flows since such a reconstruction technique cannot cope with a concentration density function with multiple maxima.

6. Application to the English Channel and southern North Sea

In this section, the methods described above are applied to the study of the advection–dispersion of the technetium-99 (^{99}Tc) in the English Channel and the southern North Sea. ^{99}Tc has a half-life of 217 000 years and its dominant source in the southern and eastern North Sea is the nuclear fuel reprocessing plant at Cap de La Hague. For this study, ^{99}Tc is, hence, supposed to behave conservatively and other sources are ignored.

The fate of this pollutant is simulated by means of the three-dimensional, hydrodynamic model of the North Western European Continental Shelf developed at the GHER (GeoHydrodynamics and Environment Research laboratory, University of Liège). This model is baroclinic and includes a robust and versatile turbulence closure scheme (Delhez et al., 1999b). It covers the whole shelf to the east of the 200 m isobath, from 48°N to 61°N, including the Skagerrak and Kattegat, with an horizontal resolution of 10′ in longitude and latitude, i.e. about 10×16 km, and 10 vertical σ levels (Delhez and Martin, 1992). The numerical implementation is based on a finite volume approach and uses a TVD scheme with superbee limiter for the advection of scalar quantities (James, 1996). The model is forced at its open ocean boundaries, which are located far away from the region of interest, by nine tidal constituents and the inverse barometer effect. The meteorological forcing data (six-hourly air temperature, surface pressure, relative humidity, wind speed, cloud cover; horizontal resolution $1.5 \times 1.5°$) are extracted from the NCEP/NCAR reanalysis of surface data from NOAA/CDC (http://www.cdc.noaa.gov/cdc/reanalysis/).

The simulations span a period of 6 years starting on the first of January 1983 from adjusted climatological mean winter fields and zero ^{99}Tc concentration. The real monthly mean release rates of ^{99}Tc given by the French COGEMA[1] operating the plant (Fig. 4) are used. The low-level radioactive sewage is released 1–2 h after local high tide.

[1] COGEMA: Compagnie Générale des Matières Nucléaires, P.O. Box 508, F 50105 Cherbourg Cedex.

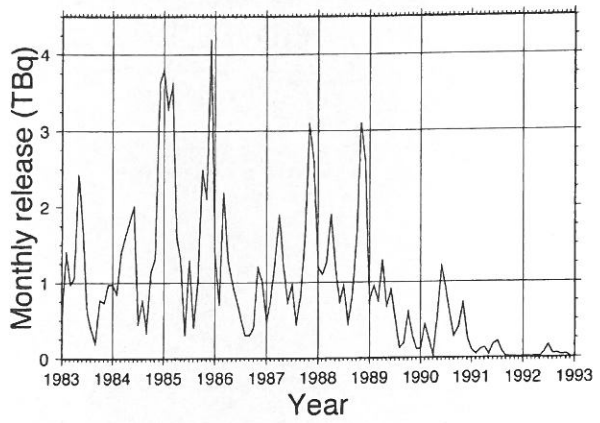

Fig. 4. Monthly release of ^{99}Tc into English Channel at La Hague.

Figs. 5 and 6 show snapshots of, respectively, the concentration field and the mean age of the ^{99}Tc at the surface computed directly from Eqs. (4) and (5). For this simulation, the initial age of the technetium is assumed to be zero when it is leaves the outfall pipe at La Hague. As a result, the mean age depicted in Fig. 6 indicates the mean time spent by the ^{99}Tc parcels since their release into the marine system.

Figs. 5 and 6 must be analyzed in two steps to avoid any misunderstanding. First, the concentration field (Fig. 5) reflects the direction of the general circulation and of the lateral spreading of the water mass tagged by the technetium. Then, the mean age can be used to infer the rate of transport (by both advection and diffusion) of the ^{99}Tc through the shelf region. As shown by Eq. (17), one should never draw conclusions about the direction of the flow from the analysis of the mean age field.

The distribution of ^{99}Tc results from the residual flow which is nearly constantly directed from the English Channel towards the North Sea (e.g. Otto et al., 1990; Delhez, 1996.) through the Strait of Dover (Fig. 7). Fig. 5 shows also that Channel waters take part in the large cyclonic motion taking place in the whole basin of the Southern Bight of the North Sea.

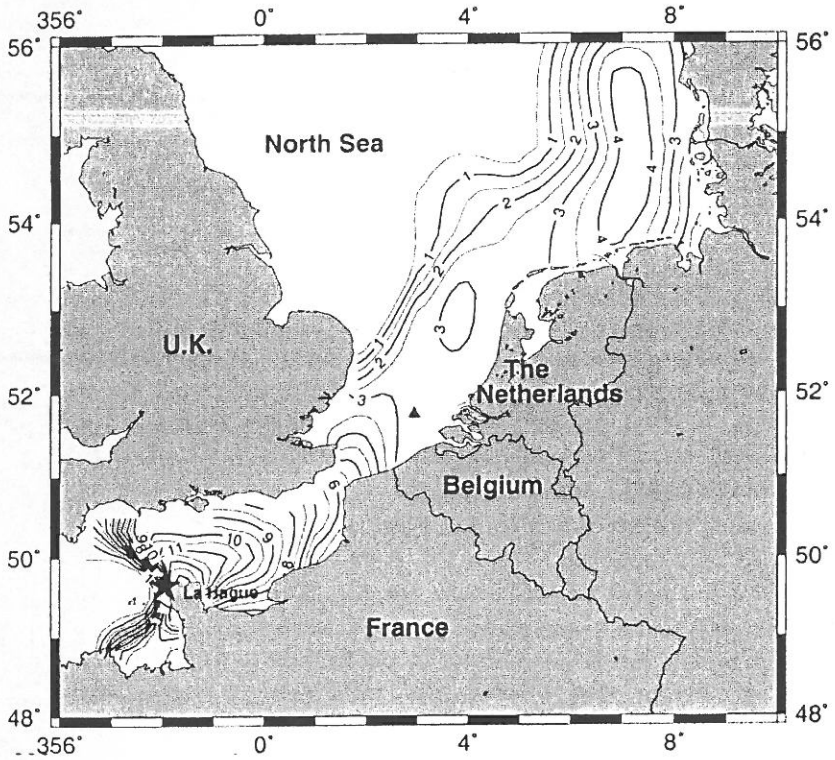

Fig. 5. Surface concentration of ^{99}Tc (in Bq/m^3) in the English Channel and the southern North Sea as simulated on March 22, 1985. The location of the release point is identified by a star (★). The filled triangle (▲) indicates the station at which particular results are displayed in Figs. 7 and 9.

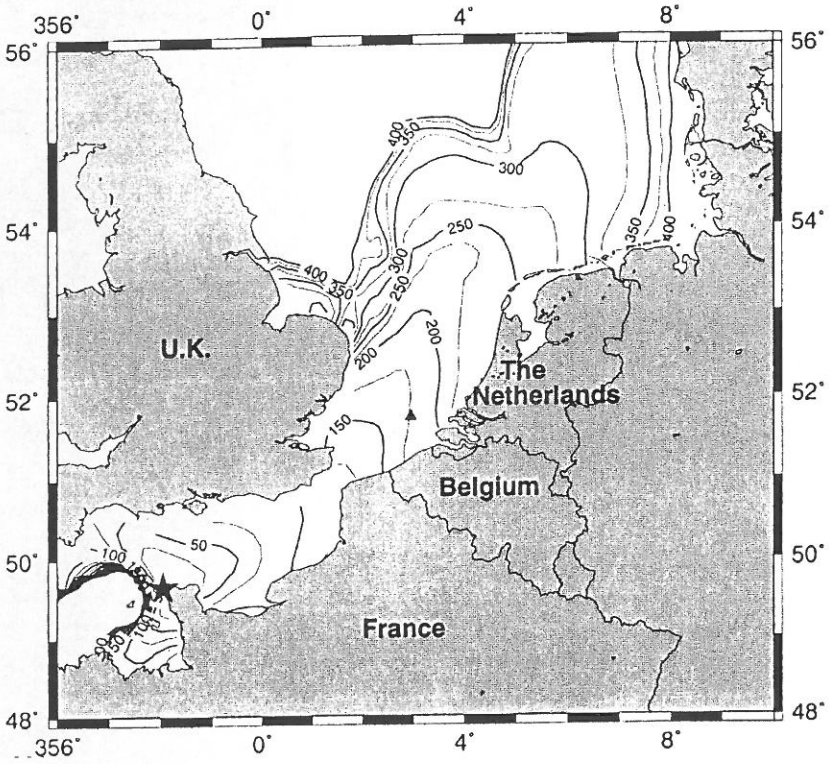

Fig. 6. Surface value of the mean age of the ^{99}Tc (in days) in the English Channel and the southern North Sea as simulated on March 22, 1985.

As a result, the plume of the technetium follows the continental coast and is separated from English coastal waters by a sharp gradient.

The occurrence of a local maximum of the ^{99}Tc concentration in the German Bight follows from the varying release rate at the reprocessing plant of La Hague (Fig. 4) and of the fluctuations of the residual flow through the Strait of Dover (Fig. 7).

Fig. 6 shows that at the end of March 1985, the mean age of the ^{99}Tc present in the English channel ranged from a few days in the vicinity of the source to about 5 months at the Strait of Dover. Although the horizontal resolution of the model is rather rough for a detailed description of the complex hydrodynamics of the English Channel, it is also apparent in Fig. 6 that coastal stations in France are characterized by slightly larger mean ages than offshore. This feature is easily explained by the persistence of residual gyres along the French coast that trap the pollutants and keep them for some time in coastal areas (Guegueniat et al., 1995; Delhez, 1996).

In the North Sea, the mean age increases gradually downstream and reaches 1 year (and more) in the German Bight. The bulk of the material forming the local concentration maximum observed in this region in Fig. 5 can, therefore, be associated with the technetium released during winter and spring 1984. As the release rate decreased during the summer months (Fig. 4), a local maximum was produced and subsequently transported across the southern North Sea. In general, contaminated waters remain in the English Channel during much of spring and summer and are exported to the North Sea by winter storms.

The spatial distribution plotted in Figs. 5 and 6 are only indicative snapshots of the concentration and mean age; temporal fluctuations are superimposed on these spatial patterns. The variability of the input and of the meteorological conditions induce indeed significant temporal fluctuations as can be seen in the time series shown in Fig. 7 for a fixed station (51°45′N, 3°E; filled triangle in Fig. 5) in the

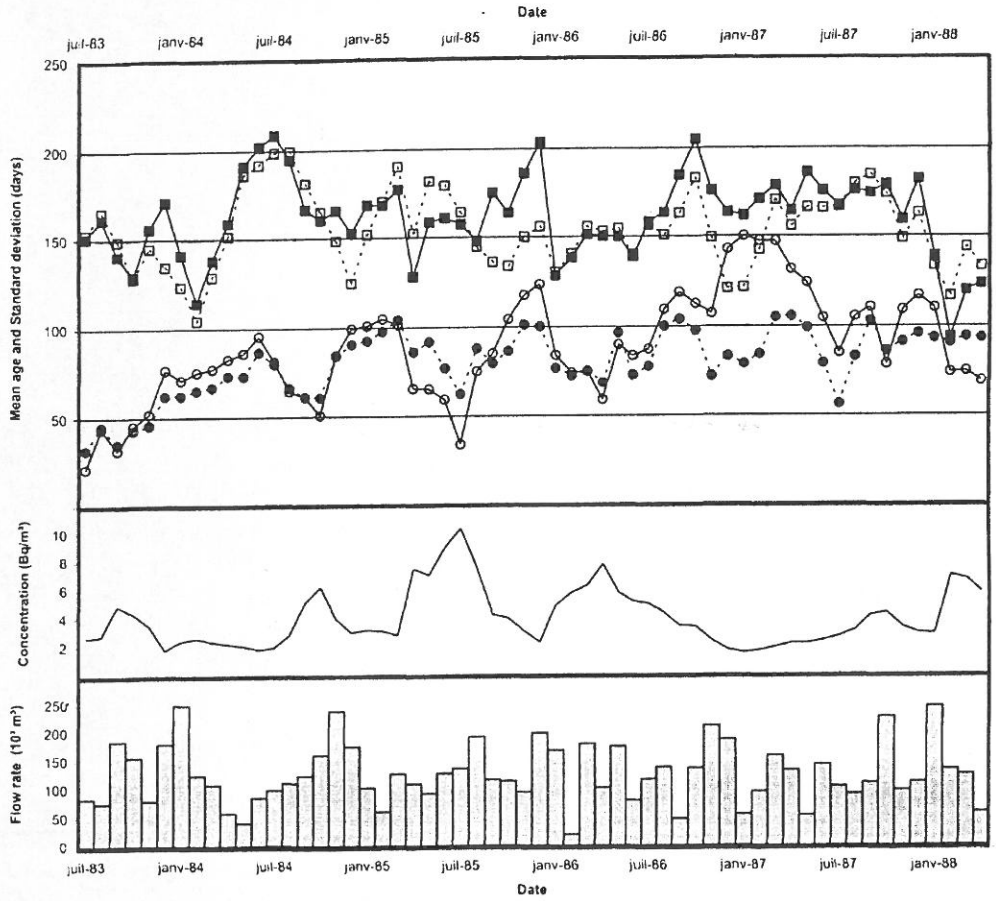

Fig. 7. Time series of selected model outputs in the Southern Bight of the North Sea (51°45′N 3°E, filled triangle in Fig. 5): mean age of the ^{99}Tc (solid line with square boxes), mean age of an artificial tracer released at Cap de La Hague (dashed line with square boxes), standard deviation of the age distribution of the ^{99}Tc (solid line with circles), standard deviation of the age distribution of the artificial tracer (dashed line with circles), concentration of the ^{99}Tc (solid line) and monthly mean flow through the Strait of Dover.

Southern Bight of the North Sea. After model spin-up, the duration of which can be approximated by the mean age, the mean age varies between 130 and 210 days. The higher values correspond to periods of reduced discharge of ^{99}Tc or to a minimum of the residual flow rate through the Strait of Dover. This flow varies indeed around a mean value of 120 000 m^3/s with peak values of more 200 000 m^3/s, particularly in fall and winter, and minimum values around 30 000 m^3/s, particularly in summer when the mean wind turns from southwest to northwest.

Fig. 6 can be compared with the mean age computed using a method presented by Salomon et al. (1995) in the same context as this application. Salomon defined the age at a location $\mathbf{x}$ as the time interval T by which the time series of the ^{99}Tc concentration at the release point $\mathbf{x}_{\text{release}}$ at Cap de La Hague has to be shifted to get the maximum cross-correlation $\theta(T)$ with the time series of the ^{99}Tc concentration at the observation point $\mathbf{x}$, i.e. the maximum of

$$\theta(T) = \frac{\langle C(t-T,\ \mathbf{x}_{\text{release}})C(t,\mathbf{x})\rangle}{\sqrt{\langle C(t,\ \mathbf{x}_{\text{release}})^2\rangle}\sqrt{\langle C(t,\ \mathbf{x})^2\rangle}} \tag{37}$$

where $\langle\cdot\rangle$ denotes the time averaging operator. The spatial distribution of this mean age computed from our results is shown in Fig. 8. This is similar to Salomon's original picture (Fig. 2 in Salomon et al.'s paper) although more smaller scale structures appear in the

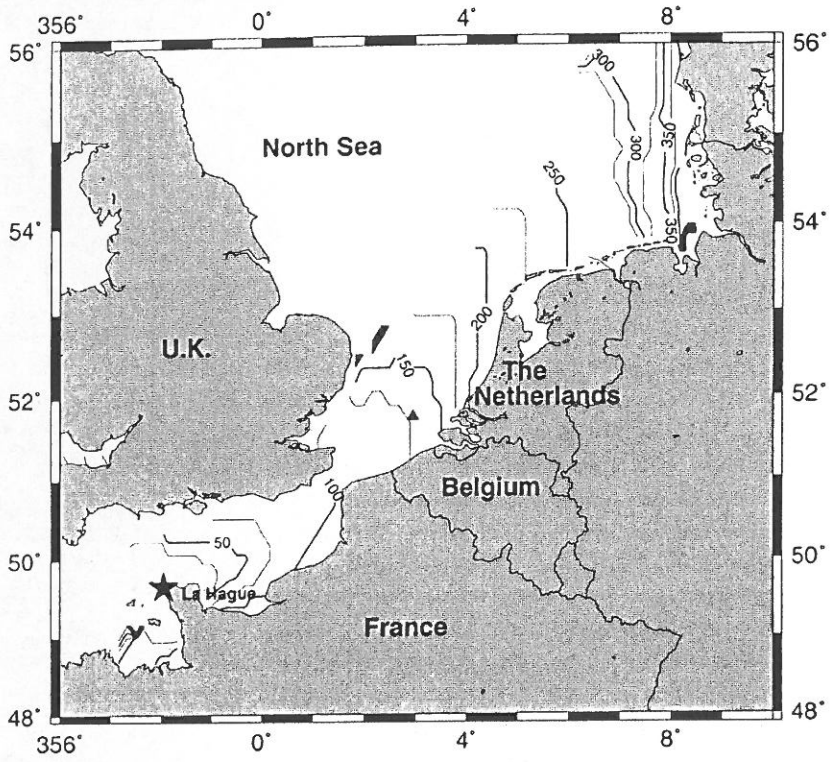

Fig. 8. Surface value of age (in days) computed from a 5-year simulation of the advection/dispersion of the ^{99}Tc using the method introduced in Salomon et al. (1995). Only the locations were the cross-correlation function is larger than 0.75 are considered.

original paper because of the finer horizontal resolution used. While Figs. 6 and 8 present similar large-scale patterns, the distributions differ, however, very much quantitatively from each other with Salomon's method consistently underestimating the age of the technetium.

One of the difficulties for the application of Salomon's method is that the maximum of the cross-correlation function is generally poorly defined because the spreading/diffusion of the tracer in its way from the source to the observation point introduces a severe distortion of the time series of the concentration observed at La Hague and at the observation point. As a result, Salomon's method can only be applied to compute a mean age averaged over a period of time that is long enough for the cross-correlation to be significant. In particular, it cannot even be applied to the simple 1D analytical case with constant release considered in Section 3. As shown in Fig. 7, the seasonal variations of the mean age are, however, important characteristics of this system and should, therefore, be described as accurately as possible.

The method used by Prandle (1984) to compute the age of the ^{137}Cs discharged from La Hague and Windscale–Sellafield (Irish Sea) and transported through the European continental shelf suffers from the same limitation: it is based on the assumption of constant hydrodynamic fields so that the temporal fluctuations of the age are also neglected.

Assuming that the flow is in a steady state (Prandle uses a constant residual velocity field), Prandle sets initial conditions to zero throughout the model domain, introduces a constant rate of inflow of material and defines the age A_P of the material present within the volume V (this definition was formulated originally for depth-integrated studies but is adapted here to three dimensions) by

$$A_P = \int_0^\infty \frac{\iiint_V \frac{\partial C}{\partial t}(t,\ \mathbf{x})\mathrm{d}V}{\iiint_V C(\infty,\ \mathbf{x})\mathrm{d}V} t\mathrm{d}t \tag{38}$$

where $C(\infty, \mathbf{x})$ denotes the concentration field at $t \to \infty$. This definition amounts to define the local value of the age by

$$a_P(\mathbf{x}) = \int_0^\infty \frac{\frac{\partial C}{\partial t}(t, \mathbf{x})}{C(\infty, \mathbf{x})} t\mathrm{d}t \tag{39}$$

The mean ages reported by Prandle for the material discharged from Cap de la Hague are about two times larger than the values computed in this study and by Salomon et al. (1995). A possible reason for this overestimation of the mean age could be the use by Prandle of a constant residual transport field that misses all the fluctuations of the flow through the Strait of Dover (Fig. 7).

Interestingly, Prandle's method can be seen as a particular case of the method introduced by Delhez et al. (1999a). Prandle's method amounts indeed to the definition of an artificial tracer, released at a constant rate, whose age $a(t, \mathbf{x})$ can be evaluated at any time t using Eq. (3), where $c(t, \mathbf{x}, \tau)$ is the concentration distribution function of this artificial tracer. If, following Hirst (2000), one takes into account that the release starts at $t=0$, i.e. that no material in the system is older than $\tau = t$ at time t, and that the concentration distribution function is time-invariant for $\tau \leq t$ under the assumption of constant hydrodynamics and discharge rate, one gets:

$$c(t, \mathbf{x}, \tau) = c(\infty, \mathbf{x}, \tau)h(t - \tau) \tag{40}$$

where $h(\cdot)$ is the Heaviside step function. Consequently, the concentration and age of the artificial tracer are given respectively by

$$C(t, \mathbf{x}) = \int_0^t c(\infty, \mathbf{x}, \tau)\mathrm{d}\tau \tag{41}$$

and

$$a(t, \mathbf{x}) = \frac{1}{C(t, \mathbf{x})} \int_0^t c(\infty, \mathbf{x}, \tau)\tau\mathrm{d}\tau \tag{42}$$

Therefore,

$$\frac{\partial}{\partial t} C(t, \mathbf{x}) = c(\infty, \mathbf{x}, t) \tag{43}$$

and the age of the material released from the initial time to the time t can be computed from the time series of the tracer concentration by (Hirst, 2000)

$$\begin{aligned} a(t, \mathbf{x}) &= \frac{1}{C(t, \mathbf{x})} \int_0^t c(\infty, \mathbf{x}, \tau)\tau\mathrm{d}\tau \\ &= \frac{1}{C(t, \mathbf{x})} \int_0^t \frac{\partial C(\tau, \mathbf{x})}{\partial \tau} \tau\mathrm{d}\tau \end{aligned} \tag{44}$$

Taking $t \to \infty$ in Eq. (44), Eq. (39) follows immediately.

The analysis of the age field can be pursued by computing the concentration distribution function. Here, the method described at the end of Section 4 is used to solve the five-dimensional equation for the concentration distribution function with a resolution $\Delta\tau$ of 30 days in the age direction for a total of height age classes (i.e. $N=8$) describing in detail the part of the age spectrum from $\tau = 0-240$ days. The total concentration field provides basic information about the tail of the spectrum, i.e. for $\tau > 240$ days.

Fig. 9 shows two snapshots of the concentration distribution function of the ^{99}Tc in the Southern Bight of the North Sea in Spring 1985. The two panels show clearly that the material present at this location is made of tracer parcels that were discharged at Cap de La Hague at various past moments. On the 22nd of March, the tail of the spectrum corresponding to ages larger than 240 days represents a significant proportion of the material at this location. On the 21st of April, however, the largest part of the age spectrum is well covered by the height age classes used in the computation. Between these two moments, the concentration of the ^{99}Tc increased rapidly and this is reflected in the concentration distribution function that shows that the material is getting younger. The mean age drops from 177 days at the end of March to 129 days at the end of April. In the same time, the standard deviation is reduced by about the same amount from 102 to 62 days. A systematic comparison of the time series of the mean age and of the standard deviation (not shown) reveals the same features. Because the flow through the English Channel is basically one-dimensional, any significant increase of the local concentration occurs through the advection–diffusion of younger material and contributes to the decrease of

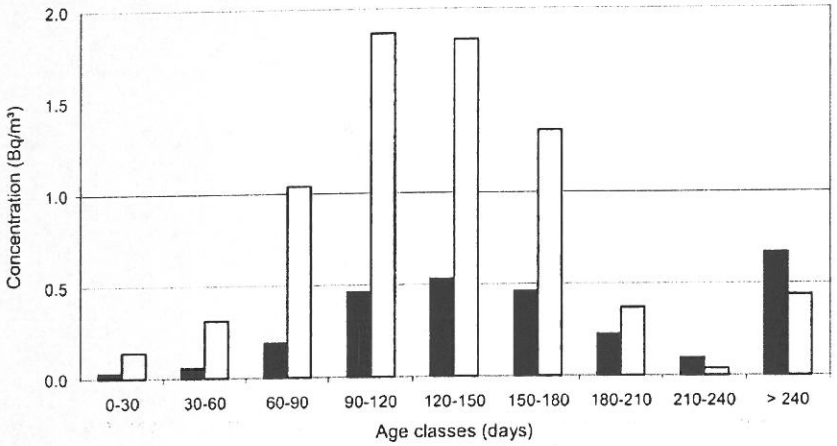

Fig. 9. Distribution of the concentration of the ^{99}Tc among the different age classes. Results for a point in the Southern Bight of the North Sea (cf. Fig. 5 for exact location) on the 22nd of March 1985 (black bars) and the 21st of April 1985 (white bars).

both the mean age and its standard deviation. On the contrary, at least on time scales shorter than the advective transport from the source, any reduction of the concentration is accompanied by a relative increase of the fraction of older material and, hence, by an increase of the mean age and of the standard deviation of the age distribution.

The mean ages corresponding to the snapshots shown in Fig. 9 are both larger than the age provided by the method of Salomon et al. (1995) at this location, i.e. about 135 days. As shown in Fig. 7, this is also the case at most other moments. More generally, the age given by Eq. (37) underestimates the age of the ^{99}Tc at nearly every location and moments. Fig. 9 helps to understand why. Let us consider the case of a massive release of ^{99}Tc at La Hague during a given period of time. This patch is transported through the English Channel and the Southern Bight of the North Sea. As this transport occurs mainly through advection, the time series of the concentration at the observation point will reflect the time series of the concentration at the release point with some delay and with a significant reduction of the maximum concentration induced by the horizontal diffusion. What the computation of the cross-correlation provides is basically the delay between the relative maxima of the two time series (because lower concentrations contribute very little to the cross-correlation). Therefore, the age given by the method of Salomon et al. (1995) will correspond to an average advection time scale. This is, therefore, a rather poor diagnostic of the real transport of material through the system as it does not take into account the numerous diffusion processes. As shown before, the diffusion is responsible for the creation of the tail of the concentration distribution function and of its related asymmetry. Therefore, ignoring the diffusion amounts to neglect the older age classes and introduces a systematic bias towards younger ages. As confirmed by the comparison of the two snapshots in Fig. 9, this bias is particularly significant when the local concentration goes through a minimum, i.e. when the asymmetry of the concentration distribution function is large. On the contrary, the difference between the two ages is smaller when the concentration reaches a maximum and the old material contributes little to the actual concentration.

When building interpretations of the age field, it must be kept in mind that the age of the technetium shown in Fig. 6 is not equal to the age of the English Channel water, for instance, and it is even not equal to the age of the other radioactive effluents discharged in La Hague together with the technetium (Deleersnijder et al., 2001a). The reason is that the age field analyzed so far reflects both the variations of the hydrodynamics and of the discharge rate. Obviously, different discharge scenarios will produce different (normalized) concentration distribution functions and different age statistics. Therefore, the concentration distribution function tells us about the (temporal) origin of the material that is present at a given location at a given time but not about the time needed to travel from the source to the observation point.

To focus on the hydrodynamics and to be able to draw general conclusions about transport routes and rates, it is necessary to replace the varying discharge of the real tracer by a constant source (of unit strength) of an artificial tracer. The concentration distribution function $c^0(t, \mathbf{x}, \tau)$ of this new tracer is then nothing but the Green function of the problem. The knowledge of $c^0(t, \mathbf{x}, \tau)$ is sufficient to compute the concentration distribution function $c(t, \mathbf{x}, \tau)$ of any tracer released at Cap de La Hague at a rate $J(t)$. One has indeed

$$c(t,\ \mathbf{x},\ \tau) = J(t-\tau)c^0(t,\ \mathbf{x},\ \tau) \tag{45}$$

so that, for instance,

$$C(t,\ \mathbf{x}) = \int_0^\infty J(t-\tau)c^0(t,\ \mathbf{x},\ \tau)\mathrm{d}\tau = \int_{-\infty}^{t} J(\xi)c^0(t,\ \mathbf{x},\ t-\xi)\mathrm{d}\xi \tag{46}$$

The mean age and the higher moments of the age distribution can be computed using similar expressions.

Conversely, it is also theoretically possible to extract information about $c^0(t, \mathbf{x}, \tau)$ from the concentration distribution function $c(t, \mathbf{x}, \tau)$ of a real tracer with known discharge rate. If $c(t, \mathbf{x}, \tau)$ can be reconstructed from numerical simulations or direct measurements (using zero, first- and second-order moments and Eq. (34), for instance), then Eq. (45) can be used to infer conclusions about $c^0(t, \mathbf{x}, \tau)$ and, hence, the underlying hydrodynamics and transport rates.

The results of the simulation of a constant unit discharge at Cap de La Hague are shown in Figs. 7 and 10. The differences between the age of this artificial tracer and that of the technetium are of the order of 10–20 days only during a large part of the simulation but reaches 50 days when sharp variations of the discharge rate of the technetium occur. Globally, the age of the artificial tracer tends to be larger (resp. smaller) than the age of the technetium when this shows a relative minimum (resp. maximum) associated with an increase (resp. a decrease) of the discharge rate. This is of course due to the influence of older technetium parcels being larger at decreasing and low concentration.

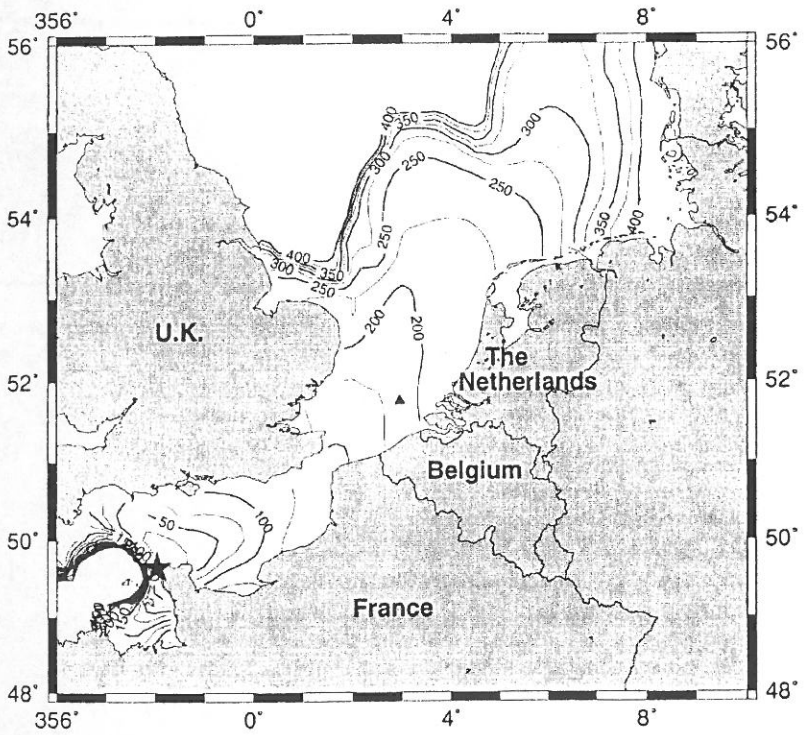

Fig. 10. Mean age of an artificial tracer released at a constant rate at Cap de La Hague. Surface value on the 22nd of March 1985 (in days).

Once again, the age of the artificial tracer is more than an advective time scale of the system. It forms an integrated image, synthesising both the advection and the dispersion processes acting in the system and is not merely a modified picture of the residual flow through the Strait of Dover. This flow is of course a major characteristics of the system but its influence on the age occurs only through its average value over a period of time of the order of the age itself, making the relationship between both variables rather complex (cf. Fig. 7). Moreover, the age takes also into account the diffusion and all the other processes, like tidal oscillations and high frequency wind induced currents, that contributes to a spatial spreading of the patches. This is what makes of the age such an interesting diagnostic tool.

The computation of the standard deviation of the concentration distribution function can be used to assess and highlight the part played by diffusion processes. Let us indeed consider again the 1D analytical example used in Section 3 together with the equations for the higher-order moments of the age distribution. At the steady state, these moments verify the coupled equations

$$\begin{cases} u\dfrac{\mathrm{d}\mu_0}{\mathrm{d}x} = 0 + \kappa\dfrac{\mathrm{d}^2\mu_0}{\mathrm{d}x^2} \\ u\dfrac{\mathrm{d}\mu_1}{\mathrm{d}x} = \mu_0 + \kappa\dfrac{\mathrm{d}^2\mu_1}{\mathrm{d}x^2} \\ u\dfrac{\mathrm{d}\mu_2}{\mathrm{d}x} = 2\mu_1 + \kappa\dfrac{\mathrm{d}^2\mu_2}{\mathrm{d}x^2} \end{cases} \tag{47}$$

With the boundary conditions

$$\mu_0(0) = C_0, \quad \mu_1(0) = 0, \quad \mu_2(0) = 0 \tag{48}$$

describing the characteristics of the source at $x=0$, one gets easily

$$\begin{cases} \mu_0(x) = C_0 \\ \mu_1(x) = C_0\dfrac{x}{u} \\ \mu_2(x) = 2C_0\dfrac{\kappa x}{u^3} + C_0\dfrac{x^2}{u^2} \end{cases} \tag{49}$$

or

$$C(x) = C_0, \quad a(x) = \frac{\mu_1(x)}{\mu_0(x)} = \frac{x}{u},$$
$$\sigma = \sqrt{\frac{\mu_2(x)}{\mu_0(x)} - a(x)^2} = \sqrt{\frac{2\kappa x}{u^3}} \tag{50}$$

Hence, while the mean age does not depend on diffusion, the standard deviation σ of the age distribution provides a direct image of the diffusion coefficient.

In real three-dimensional applications, the dynamics of the age, of its average value and of its standard deviation are of course more complex so that Eq. (50) is no more valid. It is clear, however, that the occurrence of particles of different ages simultaneously present at a given location can only be produced by the mixing of different water masses, i.e. by diffusion. This suggests that the standard deviation of the age distribution is an integrated measure of the level of mixing undergone by a water parcel along its way from the source to the observation point.

In spite of the crudeness of the simplifications used to derive Eq. (50), the value of these analytical results are demonstrated by the statistics obtained for the artificial tracer released at Cap de La Hague (Fig. 11). On the one hand, the mean age increases nearly linearly with the downstream coordinate in the eastern basin of the English Channel and in the Southern Bight of the North Sea. On the other hand, the standard deviation of the age distribution shows a more gentle increase, in agreement with Eq. (50). The situation is more complex further downstream, in the Central North Sea and the German Bight, as the structure of the flow becomes more and more two- or three-dimensional.

At this point, one word of caution is necessary. When interpreting the standard deviation of the age distribution as a measure of diffusion, one should always keep in mind that diffusion means here all the processes that contribute to the mixing of different particles to form a water parcel. For the system under study, this covers not only the molecular diffusion and the "true" turbulent diffusion but also all the motions characterized by time-scales smaller than a fortnight. In particular, it is clear that the oscillations of the tidal and wind-induced currents and their vertical shear dominate the mixing so that the explicit diffusion coefficient used in the model does not provide a

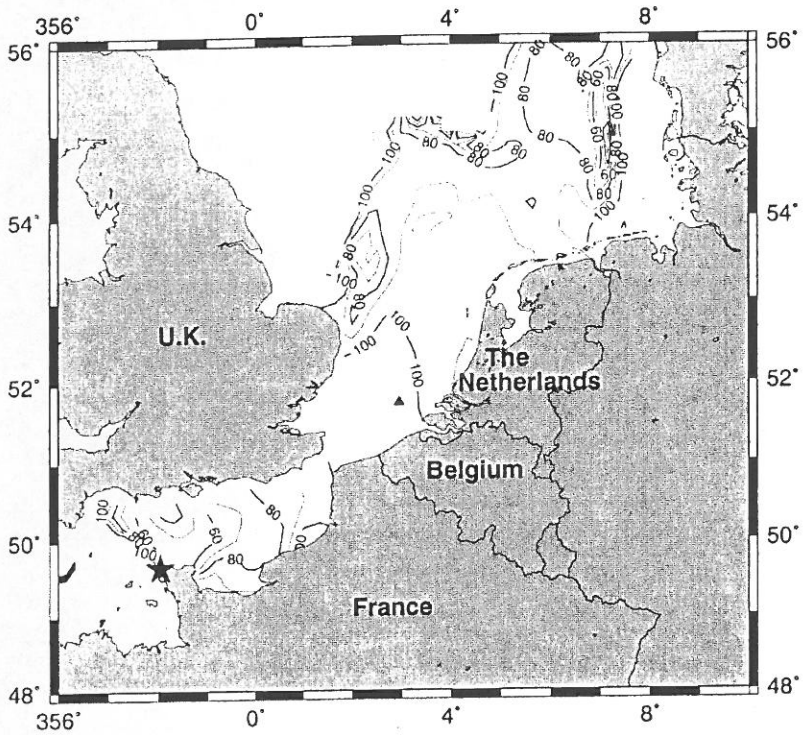

Fig. 11. Standard deviation of the age distribution of an artificial tracer released at a constant rate at Cap de La Hague. Surface value on the 22nd of March 1985 (in days).

reasonable gauge of the level of diffusion acting in the system. The standard deviation of the age distribution does provide such a gauge and is, therefore, particularly valuable.

Fig. 7 shows also that the statistics exhibit significant temporal fluctuations (for completeness, the statistics relating to the technetium-99 are also shown.). In general, the mean and the standard deviation evolve in phase as any reduction of the flux of new material to the observation point induces an increase of the age and a larger spreading of the age distribution during a transition phase before much of the older material is removed. In contrast, the raising of the concentration goes together with a reduction of the mean age and creates a well-defined maximum of the age distribution.

7. Conclusion

The determination of the mean age of the water or of a tracer is a valuable tool to quantify the transport through the marine system. It provides indeed a synthesis to assess both the advection and diffusion acting in this system. In numerical models, this diagnostic is particularly flexible as artificial tracers can be defined to match any particular need or interest. With previous methods of computation, the real meaning of the mean age is not clear among others because, like the radio-age (Deleersnijder et al., 2001a), they combine the ages of different tracers into one single measure. In this respect, the general theory of age developed in Delhez et al. (1999a) offers a clear and unambiguous definition of the age of a tracer.

Numerical experiments of the simulation of the fate of the technetium-99 released in the English Channel at Cap de La Hague show that the general theory is also superior to the previous methods (e.g. Prandle, 1984; Salomon et al., 1995) as it describes both the temporal and spatial fluctuations of the mean age.

The mean age provides, however, only a rough description of the real age structure, i.e. of the distribution of the age of the different particles that make up the water parcel. Here also the concept of

concentration distribution function offers much clarification.

In this paper, the numerical aspects associated with the resolution of the differential equation of the concentration distribution function in a five-dimensional space (time 3D space age space) have been developed. The method provides an exact integration of the ageing term and amounts to the simulation of the advection/dispersion of as many artificial tracers as the number of age classes retained in the analysis.

The computation of the higher-order moments of the age distribution can also be used to supplement the knowledge of the mean age. These higher-order moments have been shown to satisfy coupled partial differential equations complementing the general theory set out in Delhez et al. (1999a) and Deleersnijder et al. (2001a). The equations can be solved for the moments up to any order with usual integration techniques for active tracers.

Numerical experiments in the English Channel show that the spreading of the ages of the particles of technetium-99 present in a water parcel is large and varies with time as the result of the variations of the release rate and of the flow. As the width of the age spectrum results from mixing, it is proposed that the standard deviation of the age distribution be used as an integrated measure of the diffusion processes acting in the system. Therefore, the age statistics, initially introduced to measure the advection only, can also be used to quantify the level of diffusion.

Acknowledgements

E.J.M. Delhez and E. Deleersnijder are Research Associates with the Belgian National Fund for Scientific Research. Part of the present work was carried out when E. Deleersnijder was a Chargé de Recherche CNRS at Rennes' Institut de Recherche Mathématique. The authors are indebted to NOAA/CDC and Franck Dumas (Ifremer) for providing data to force the technetium-99 simulations.

References

Beckers, J.-M., Delhez, E.J.M., Deleersnijder, E., 2001. Some properties of generalised age-distribution equations in fluid dynamics. SIAM Journal on Applied Mathematics 61 (5), 1526–1544.

Beining, P., Roether, W., 1996. Temporal evolution of CFC11 and CFC12 concentrations in the ocean interior. Journal of Geophysical Research 101, 16455–16464.

Bolin, B., Rodhe, H., 1973. A note on the concepts of age distribution and transit time in natural reservoirs. Tellus 25, 58–62.

Broecker, W.S., Peng, T.-H., Trumbore, S., Bonami, G., Wolfi, W., 1990. The distribution of radiocarbon in the Glacial Ocean. Global Biogeochemical Cycles 4, 103–107.

Campin, J.-M., Fichefet, T., Duplessy, J.-C., 1999. Problems using radiocarbon to infer ventilation rates for past and present climates. Earth and Planetary Science Letters 165, 17–24.

Dahlgaard, H., 1995. Transfer of European coastal pollution to the Arctic: radioactive tracers. Marine Pollution Bulletin 31 (1–3), 3–7.

Deleersnijder, E., Campin, J.-M., Delhez, E.J.M., 2001a. The concept of age in marine modelling: I. Theory and preliminary model results. Journal of Marine Systems 28, 229–267.

Deleersnijder, E., Delhez, E.J.M., Crucifx, M., Beckers, J.M., 2001b. On the symmetry of the age field of a passive tracer released into a one-dimensional fluid flow by a point-source. Bulletin de la Société Royale des Sciences de Liège 70 (1), 5–21.

Delhez, E.J.M., 1996. Reconnaissance of the general circulation of the North-Western European Continental Shelf by means of a three-dimensional turbulent closure model. Earth-Science Reviews 41, 3–29.

Delhez, E.J.M., Carabin, G., 2001. Integrated modelling of the Belgian Coastal Zone. Estuarine Coastal and Shelf Science, in press.

Delhez, E.J.M., Martin, G., 1992. Preliminary results of 3D baroclinic numerical models of the mesoscale circulation on the North-Western European Continental Shelf. Journal of Marine Systems 3, 423–440.

Delhez, E.J.M., Campin, J.-M., Hirst, A.C., Deleersnijder, E., 1999a. Toward a general theory of the age in ocean modelling. Ocean Modelling 1, 17–27.

Delhez, E.J.M., Grégoire, M., Nihoul, J.C.J., Beckers, J.M., 1999b. Dissection of the GHER turbulence closure scheme. Journal of Marine Systems 21, 379–397.

England, M.H., 1995. The age of water and ventilation timescales in a global ocean model. Journal of Physical Oceanography 25, 2756–2777.

England, M.H., Holloway, G., 1998. Simulations of CFC content and water mass age in the deep North Atlantic. Journal of Geophysical Research 103 (C8), 15885–15901.

Gueguenia t, P., Bailly du Bois, P., Salomon, J.-C., Masson, M., Cabioch, L., 1995. FLUXMANCHE radiotracers measurements: a contribution to the dynamics of the English Channel and North Sea. Journal of Marine Systems 6, 483–494.

Hall, T.M., Plumb, R.A., 1994. Age as a diagnostic of stratospheric transport. Journal of Geophysical Research 99, 1059–1070.

Haine, T.W.N., Watson, A.J., Liddicoat, M.I., Dickson, R.R., 1998. The flow of Antarctic bottom water to the southwest Indian Ocean estimated using CFCs. Journal of Geophysical Research 103/C12, 27637–27653.

Hirst, C.A., 2000. Determination of water component age in ocean models: application to the fate of North Atlantic Deep Water. Ocean Modelling 1 (2–4), 81–94.

Holzer, M., Hall, T.M., 2000. Transit time and tracer-age distribution in geophysical flows. Journal of Atmospherical Sciences 57, 3539–3558.

James, I.D., 1996. Advection schemes for shelf sea models. Journal of Marine Systems 8, 237–254.

Jenkins, W.J., 1987. Studying subtropical thermocline ventilation and circulation using tritium and ^{3}He. Journal of Geophysical Research 103/C15, 15817–15831.

Jenkins, W.J., Clarke, W.B., 1976. The distribution of ^{3}He in the western Atlantic Ocean. Deep-Sea Research 23, 481–494.

Khatiwala, S., Visbeck, M., Schlosser, P., 2001. Age tracers in an Ocean GCM. Deep Sea Research, Part I 48, 1423–1441.

Ostlund, G., 1994. Isotope tracing of Siberian river water in the Arctic Ocean. Journal of Environmental Radioactivity 25 (1–2), 57–63.

Otto, L., Zimmerman, J.T.F., Furnes, G.K., Mork, M., Saetre, R., Becker, G., 1990. Review of the physical oceanography of the North Sea. Netherlands Journal of Sea Research 26 (2–4), 161–238.

Prandle, D., 1984. A modelling study of the mixing of ^{137}Cs in the seas of the European continental shelf. Philosophical Transactions of the Royal Society of London, Series A 310, 407–436.

Rutgers Van der Loeff, M.M., Key, R.M., Scholten, J., Bauch, D., Michel, A., 1995. ^{228}Ra as a tracer for shelf water in the Arctic Ocean. Deep-Sea Research, Part II 42 (6), 1533–1553.

Salomon, J.C., Breton, M., Gueguenia t, P., 1995. A 2D long term advection–dispersion model for the Channel and southern North Sea—Part B: transit time and transfer function from Cap de la Hague. Journal of Marine Systems 6, 515–527.

Takeoka, H., 1984. Fundamental concepts of exchange and transport time scales in a coastal sea. Continental Shelf Research 3, 326–331.

Thiele, G., Sarmiento, J.L., 1990. Tracer dating and ocean ventilation. Journal of Geophysical Research 95 (C6), 9377–9391.

Tou, J.T., Gonzalez, R.C., 1974. Pattern Recognition Principles. Addison-Wesley Publishing Company—Advanced Book Program, Reading, Massachusetts, 377 pp.

Turekian, K.K., Tanaka, N., Turekian, V.C., Torgersen, T., Deangelo, E.C., 1996. Transfer rates of dissolved tracers through estuaries based on ^{228}Ra: a study of Long Island Sound. Continental Shelf Research 16 (7), 863–873.

Zimmerman, J.T.F., 1976. Mixing and flushing of tidal embayments in the western Dutch Wadden Sea — Part I: distribution of salinity and calculation of mixing time scales. Netherlands Journal of Sea Research 10 (2), 149–191.